Fluorescence Depolarization of *cis*- and *trans*-Parinaric Acids in Artificial and Red Cell Membranes Resolved by a Double Hindered Rotational Model†

Teresa M. Calafut, James A. Dix, and A. S. Verkman*

Division of Nephrology, Cardiovascular Research Institute, University of California, San Francisco, California 94143-0532

Received January 3, 1989; Revised Manuscript Received March 6, 1989

ABSTRACT: Although steady-state anisotropy measurements of phase-sensitive probes provide a qualitative description of the phase behavior of biomembranes, there is little information about the physical state of lipid domains. We have developed a ground-state double hindered rotator model (DHR) for fluorescence anisotropy decay, in which probes possess separate rotational correlation times and r_∞ in each phase. To validate the model, multifrequency differential phase angles (Δ) and modulation amplitudes (Λ) were measured in a two-compartment cuvette with combinations of POPOP, TMA-DPH, and DPH in isotropic solvents and in DPPC liposomes. Rotational parameters obtained by fitting the DHR model were similar to those of a single hindered rotator model fitted to data obtained separately for each probe. As predicted by the model, negative Δ and decreasing Λ with increasing modulation frequency were obtained when fluorophores in isotropic solvents were paired with fluorophores in DPPC liposomes. The rotational parameters of the phase-sensitive fluorophores *cis*-parinaric (cPnA) and *trans*-parinaric (tPnA) acid in DPPC/DMPC (1:0, 0:1, and 1:1) liposomes were determined at 15–40 °C. Two lifetimes (1 and 3 ns) were obtained above the phase transition temperature (T_c); >95% of the fluorescence intensity was described by two lifetimes (3–9 and 12–32 ns) below T_c. Negative Δ values were obtained when solid-phase lipid was present. r_∞ varied from 0.26–0.32 below to 0.11–0.14 above T_c; at intermediate T, where two phases coexists, r_∞ values were ~0.23 and ~0.31. These data indicate very hindered PnA rotation in solid-phase lipid. In red cell ghost membranes, r_∞ values were 0.07–0.13. These results establish the application of ground-state rotational heterogeneity to describe fluorophore rotation in membranes having more than one lipid-phase environment.

Measurements of the fluorescence anisotropy of lipophilic fluorophores are useful in examining the fluidity properties of membranes. Parinaric acids are particularly sensitive to the membrane phase state; *cis*-parinaric acid (cPnA)[1] partitions equally between gel and fluid phases while *trans*-parinaric acid (tPnA) preferentially partitions into the gel-phase lipid (Sklar, 1980; Sklar et al., 1979a,b). There are large differences in parinaric acid lifetimes in gel- and fluid-phase lipid (Parasassi et al., 1984); however, little is known about the time-resolved rotational motion of these probes in the lipid environment.

Although steady-state anisotropy measurements have provided important information about changes in the membrane phase state, time-resolved anisotropy decay measurements are essential to obtain a detailed description of probe rotation in individual lipid environments. Measurement of anisotropy decay by multifrequency differential polarization using the phase-modulation technique gives decay parameters that are similar to those obtained by pulse methods (Lakowicz et al., 1984).

Models of anisotropy decay that have been applied to study fluorophore rotations are based on the presence of a single fluorescent species rotating isotropically, anisotropically, or in a hindered environment (Lakowicz et al., 1985). In a membrane consisting of coexistent gel and fluid phases, fluorophore signals arise from two distinct environments in which fluorophore rotation would, in general, be quite different. Therefore, we have developed and applied to artificial and real systems a double hindered rotator model having ground-state rotational heterogeneity which describes fluorophore motion in terms of two independently rotating species.

The application of differential polarization methods to determine parameters for the double hindered rotator model was validated by using the fluorophores DPH and TMA-DPH in isotropic solvents, and in DPPC liposomes. Parameters obtained from depolarization measurements of fluorophores in a homogeneous environment were compared to those obtained by using a two-compartment cuvette containing fluorophores having different rotational parameters. The double hindered rotator model was then tested with pure and mixed artificial membranes, and red cell ghosts. At temperatures where two phases coexisted, the double hindered rotator model fit the depolarization data significantly better than models describing rotation of a single fluorophore in a hindered or anisotropic environment. On the basis of a critical examination of the data, we conclude that the double hindered rotator model describes fluorophore rotations in a two-phase environment more accurately than other models but cannot yet be used to determine precisely all of the rotational parameters with a high degree of precision.

† This work was supported by NIH Grants DK35124, DK39354, and HL42368, a grant from the National Cystic Fibrosis Foundation, and a grant-in-aid from the American Heart Association. A.S.V. is an established investigator of the American Heart Association.

* Address correspondence to this author at the Cardiovascular Research Institute, University of California, 1065 Health Scienes East Tower, San Francisco, CA 94143-0532.

[1] Abbreviations: cPnA, 9,11,13,15-*cis*,*trans*,*trans*,*cis*-octadecatetraenoic acid; tPnA, 9,11,13,15-*trans*,*trans*,*trans*,*trans*-octadecatetraenoic acid; DPH, 1,6-diphenyl-1,3,5-hexatriene; TMA-DPH, 1-[4-(trimethylammonio)phenyl]-6-phenyl-1,3,5-hexatriene; DPPC, dipalmitoylphosphatidylcholine; DMPC, dimyristoylphosphatidylcholine; POPOP, 1,4-bis(5-phenyl-2-oxazolyl)benzene; SHR, single hindered rotator model; DHR, double hindered rotator model; ISO, isotropic rotator model; ANISO, anisotropic rotator model with two correlation times.

0006-2960/89/0428-5051$01.50/0

Materials and Methods

DPH, TMA-DPH, tPnA, and cPnA were obtained from Molecular Probes (Eugene, OR). DPPC was obtained from Avanti Polar Lipids Inc. (Birmingham, AL). DMPC was obtained from Sigma Chemical Co. (St. Louis, MO). Unilamellar liposomes were prepared by drying a chloroform solution of pure lipid or lipid mixture under argon. The lipid was redissolved in diethyl ether and sonicated for 20 s with a bath sonicator (Laboratory Supplies, Hicksville, NY). The lipid solution was then dried to a thin film under argon, resuspended in buffer (150 mM NaCl/5 mM Na_2HPO_4, pH 7.4) to a concentration of 25 mg/mL, and bath-sonicated for 30 min above the phase transition temperature of the lipid. Liposomes were used on the day of preparation or stored under argon overnight at 4 °C and resonicated before use. Red cell ghosts were prepared as described previously (Steck & Kant, 1974). Prior to probe incorporation, lipids were diluted to a concentration of 500 μM (for tPnA or cPnA studies) or 200 μM (for DPH or TMA-DPH studies) with argon-gassed buffer.

DPH, TMA-DPH, tPnA, or cPnA was added to lipids from stock solutions to give lipid:dye ratios of >50 (cPnA and tPnA) or >100 (DPH and TMA-DPH). Stock solutions of tPnA (5 mM in acetone), cPnA (1.25 mM in ethanol), DPH (1 mM in DMSO), and TMA-DPH (1 mM in acetone) were stored in darkened vials under argon at −80 °C. Liposomes were vortexed vigorously during addition of the probe and for 1 min afterward. Samples containing fluorescent probes were incubated in the dark above the phase transition temperature of the lipid for 30 min prior to fluorescence measurements.

Phase/Modulation Measurements. Fluorescence was measured by using an SLM 48000 fluorometer (SLM Instruments, Urbana, IL). Samples were sealed under argon in acrylic or quartz cuvettes and stirred by a Teflon-coated magnetic stirring bar. Cuvettes were placed in a thermostated cuvette holder. The two-compartment cuvette consisted of a 1 × 1 cm quartz cuvette divided into two equal chambers by a quartz divider running parallel to the face of the cuvette. The two-compartment cuvette was aligned in the sample chamber so that the excitation beam was perpendicular to the quartz divider. Temperature was controlled by a water bath heater/circulator (Haake Inc., Saddle Brook, NJ) and determined by a thermistor inserted into the cuvette and connected to a temperature monitor (Cole-Palmer 8502-25, Chicago, IL).

Lifetime and differential polarization measurements were made by using the multifrequency phase-modulation method (Lakowicz, 1985). Modulation was obtained by a Pockel's cell. Ten or more frequencies in the range 2–200 MHz were used. Fluorescence was excited at 325 nm with a HeCd laser (Liconix 4230NB, 7.5 mW at 325 nm, Sunnyvale, CA). Emitted light passed through a KV 408 low-fluorescence filter and a GG 420 glass cut-on filter for DPH and TMA-DPH, or through KV 380 and WG 345 filters for tPnA and cPnA (Schott Glass, Duryea, PA). Photomultiplier voltages ranged from 450 to 700 V with a gain of 100 for differential polarization measurements and from 350 to 500 V with a gain of 10 for the reference photomultiplier in lifetime measurements. The Pockel's cell was tuned to give modulation ratios >4 (in SLM instrument units, corresponding to ~30% modulation) for the reference photomultiplier. To reduce background noise, the photomultiplier was cooled to −10 °C by a thermoelectric cooler. The background signal from liposomes and ghosts in the absence of fluorophore was less than 2% and 4%, respectively, of the total signal intensity.

Lifetimes were referenced against POPOP in ethanol. A single POPOP lifetime of 1.35 ns was determined with a zero-lifetime glycogen reference, in agreement with that reported previously (Lakowicz et al., 1981). To eliminate polarization artifacts, lifetime measurements were performed with a vertical excitation polarizer and emission polarizer oriented at 54.3° from the vertical. Differential and steady-state polarizations were measured in the T-format. Differential phase angles (Δ) and modulation amplitude ratios (Λ) were measured at each frequency with a vertical excitation polarizer, a fixed vertical emission polarizer, and a second emission polarizer rotated between vertical and horizonatal orientations. Standard deviations were obtained by averaging six or more measurements of Δ and Λ; for each measurement, Δ and Λ were averaged over 2.5 s.

Data Analysis. Lifetime data were analyzed in terms of models having ground-state heterogeneity using software provided by SLM. Phase angles and modulation factors were used in the fitting routine; standard deviations, estimated from repeat measurements, were used as weighting factors.

Four models of anisotropy decay [$r(t)$] were fitted to the depolarization data:

(1) Isotropic rotator (ISO):

$$r(t) = r_0 \exp(-t/\tau_c) \quad (1)$$

(2) Anisotropic rotator (ANISO):

$$r(t) = r_0[g_1 \exp(-t/\tau_{c1}) + g_2 \exp(-t/\tau_{c2})] \quad (2)$$

(3) Single hindered rotator (SHR):

$$r(t) = (r_0 - r_\infty) \exp(-t/\tau_c) + r_\infty \quad (3)$$

(4) Double hindered rotator (DHR):

$$r(t) = (A + B)/(g_1 e^{-t/\tau_{f1}} + g_2 e^{-t/\tau_{f2}}) \quad (4)$$

where

$$A = g_1 e^{-t/\tau_{f1}}[r_{\infty 1} + (r_{01} - r_{\infty 1})e^{-t/\tau_{c1}}]$$

$$B = g_2 e^{-t/\tau_{f2}}[r_{\infty 2} + (r_{02} - r_{\infty 2})e^{-t/\tau_{c2}}]$$

Model parameters included rotational correlation times (τ_{ci}), anisotropy weighting factors (g_i), and limiting anisotropies ($r_{\infty i}$).[2] The g_i factors are time-independent fractional amplitudes ($g_1 + g_2 = 1$) of fluorescence signals arising from each component of anisotropy decay. Lifetimes (τ_{fi}) were determined from separate lifetime measurements in the absence of polarization effects.[3] Maximal anisotropies (r_0) of 0.39 were used for DPH and TMA-DPH (Lakowicz, 1979; Prendergast, 1981) and 0.36 for cPnA (Rujanavech et al., 1986). An r_0 for tPnA of 0.36 was determined by extrapolating the measured steady-state anisotropies of tPnA in ethylene glycol to 0 K according to the Perrin equation (Cantor & Schimmel, 1980).

[2] Steady-state anisotropy was not used in the fitting procedure to decrease by 1 the number of parameters fitted independently. Although inclusion of this additional constraint is desirable in principle, in practice inclusion of the anisotropy constraint often caused divergence in the fitting procedure, or convergence to physically unreasonable parameters with a large χ^2 value. Even in simple hindered rotational or anisotropic models, constraint of fitted parameters by steady-state anisotropy values led to poor convergence of the fitting routine, and consequently, the anisotropy constraint is not commonly used in analysis of phase/modulation data. The origin of this problem is not at present known.

[3] Because >97% of the signal was described by two lifetimes in most experiments (>94% in all experiments) when data were fitted to a three-lifetime ground-state heterogeneity model, two lifetimes were used for the rotational calculations.

Table I: Comparison of Fits to Different Models of Anisotropy Decay[a]

	Single-Compartment Cuvette								
	fitted parameters						χ^2		
probe/solvent	ISO τ_c (ns)	SHR τ_c (ns)	SHR r_∞	ANISO τ_{c1} (ns)	ANISO τ_{c2} (ns)	g_1	ISO	SHR	ANISO
POPOP/ethanol	0.17	0.17	0.001	0.17	0.17	0.18	0.98	0.96	1.08
DPH/ethanol	0.088	0.078	0.005	0.08	0.88	0.99	7.3	0.95	0.95
DPH/mineral oil	4.6	3.9	0.04	0.68	7.0	0.02	380	130	5.9
TMA-DPH/DPPC	45	0.42	0.33	0.00	75	0.07	840	26	270

	Two-Compartment Cuvette								
	fitted parameters, DHR model					χ^2			
probe/solvent	$r_{\infty 1}$	$r_{\infty 2}$	τ_{c1} (ns)	τ_{c2} (ns)	g_1	DHR	ISO	SHR	ANISO
TMA-DPH/DPPC + POPOP/ethanol	0.29 ± 0.01	0.020 ± 0.002	0.16 ± 0.10	0.12 ± 0.01	0.15 ± 0.01	3.4	4200	4200	2300
DPH/mineral oil + POPOP/ethanol	0.00 ± 0.01	0.01 ± 0.01	5.6 ± 0.2	0.06 ± 0.01	0.23 ± 0.02	2.2	947	2600	304
TMA-DPH/DPPC + DPH/ethanol	0.23 ± 0.01	0.00 ± 0.01	0.28 ± 0.02	0.29 ± 0.01	0.66 ± 0.01	10	1500	3500	200

[a] Lifetimes for the fits were 7.23 ns (TMA-DPH in DPPC), 1.35 ns (POPOP in ethanol), 9.7 ns (DPH in mineral oil), and 5.15 ns (DPH in ethanol). r_0 values were 0.39. τ_f and r_0 were held fixed during the fit. T = 25 °C.

Measured Δ and Λ values were fitted to each $r(t)$ model by the nonlinear Marquart χ^2 minimization procedure (Bevington, 1969). For each rotational model, theoretical differential phase angles (Δ_{th}) and modulation amplitude ratios (Λ_{th}) were calculated from the Fourier transform of $r(t)$ (Weber, 1977). χ^2 values were calculated as

$$\chi^2 = \sum_i(\Delta_i - \Delta_{th})^2/\sigma_i^2 + \sum_i(\Lambda_i - \Lambda_{th})^2/\sigma_i^2 \qquad (5)$$

where σ_i is the standard deviation, estimated from multiple measurements, of Δ or Λ, and the sum is over all data points. Standard deviations in fitted parameters were estimated by inversion of the weighted correlation matrix (Bevington, 1969). Significance testing of the fits to the models was done by the F test. Analysis programs were written and compiled in Microsoft QuickBASIC 4.0.

Results

Validation of the Method. Experiments were performed to examine the precision by which rotational parameters of two independent rotators could be resolved from multifrequency phase/modulation data. Data were obtained for single-component rotators separately and then for pairs of rotators, each placed separately in one compartment of a two-compartment cuvette. Depolarization data from the two-compartment cuvette were analyzed in terms of the DHR model to determine if parameters of the individual rotators could be resolved.

Table I, top, gives the parameters and χ^2 values determined for fits of three anisotropy decay models to depolarization data obtained for a single-component system. For an isotropic, unhindered rotator such as POPOP in ethanol, the fit of an isotropic rotator model gives χ^2 near unity, suggesting the absence of significant systematic artifacts in the measurement of Δ and Λ. The fit of a single hindered rotator model with r_∞ near zero gives a fit equally as good as the isotropic rotator, since these models are equivalent in the limit $r_\infty = 0$ (eq 1 and 3). Similarly, the fit of the anisotropic rotator model gave two correlation times that were equivalent and equal to the single correlation time from the single hindered rotator model.

For DPH in ethanol and mineral oil, although the anisotropic rotator model with two correlation times gives a χ^2 lower than the isotropic rotator model, one of the correlation times is of low fractional intensity. A single hindered rotator model also gives a better χ^2, but the fitted r_∞ value is near zero (0.005). These results suggest that DPH rotation in ethanol and mineral oil is described well, but not perfectly, by an isotropic rotator model. As expected, rotation of TMA-DPH in DPPC below its phase transition temperature is described best by a single hindered rotator with large r_∞.

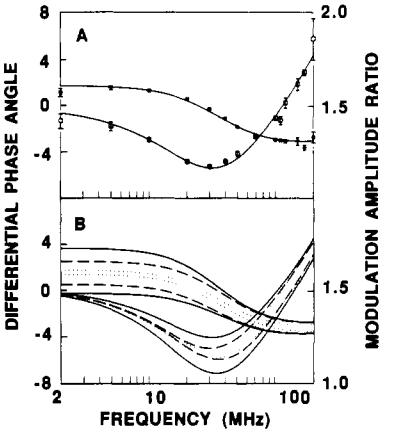

FIGURE 1: (A) Differential phase angles (O) and modulation amplitude ratios (asterisks) obtained from a two-compartment cuvette. One compartment contained 1 μM TMA-DPH/100 μM DPPC; the other compartment contained POPOP in ethanol at a concentration sufficient to give fluorescence intensity equal to the TMA-DPH sample. T = 24 °C. The lines are the least-squares fit of the DHR model to the data; parameters from the fit are given in Table I. In these and the following figures, the error bars represent standard deviations of multiple determinations (N = 6–10) of Δ and Λ. (B) Sensitivity of the fit to variations in $r_{\infty 1}$, τ_{c1}, and g_1. The least-squares fit parameters from (A) were varied by ±20%, and the frequency-dependent Δ and Λ values were simulated. Solid line, variation of $r_{\infty 1}$; dashed line, variation of g_1; dotted line, variation of τ_{c1}.

Table I, bottom, gives parameters and χ^2 values for data obtained from two single-component systems present in a two-compartment cuvette. For the three fluorophore combinations tested, χ^2 values were far better for the DHR model than for other models. Values for r_∞ obtained from the double hindered rotator model are in reasonable agreement with r_∞ values obtained for the separate samples (Table I, top). Values for τ_c are not as well determined as r_∞ values by this method. When the lifetimes of the two fluorophores used in the two-compartment cuvette are very different, τ_c values are reasonably close to those obtained when measured separately. When lifetimes of the two fluorophores are similar, however, τ_c values determined by the two methods vary greatly.

Figure 1A shows frequency-dependent Δ and Λ for the two-component system of POPOP in ethanol and TMA-DPH in DPPC obtained with the two-compartment cuvette, along with a fit of the DHR model to the data. As predicted by the

Table II: Lifetimes of cPnA and tPnA in Lipid Bilayers

probe, lipid	two-component fit				three-component fit					χ^2, no. of components		
	temp (°C)	τ_{f1} (ns)	τ_{f2} (ns)	g_1	τ_{f1} (ns)	τ_{f2} (ns)	τ_{f3} (ns)	g_1	g_2	one	two	three
Pure Lipids												
cPnA, DMPC	45	0.7	3.4	0.06	0.1	2.6	4	0.02	0.53	94	19	18
	32	3.8	9.3	0.59	1.5	5.6	34	0.04	0.08	1500	107	32
	20	3.3	12	0.16	0.6	3.7	13	0.01	0.82	542	116	128
cPnA, DPPC	45	1.3	4.4	0.10	1.3	4.4	10	0.09	0.01	33	3	4
	32	2.9	14	0.14	0.1	3.6	15	0.01	0.83	1000	161	172
	20	4.0	22	0.12	1.8	7.3	23	0.03	0.82	1500	36	25
tPnA, DMPC	45	1.8	4.7	0.52	0.01	2.5	6	0.04	0.23	270	93	69
	32	0.7	4.9	0.05	0.6	3.5	5	0.00	0.05	86	25	29
	20	4.8	23	0.14	2.3	10	28	0.04	0.69	618	32	3
tPnA, DPPC	45	1.7	4.9	0.19	0.1	3.6	8	0.03	0.23	133	5	3
	32	6.0	31	0.07	1.8	13	35	0.01	0.82	258	8	2
	20	9.0	46	0.07	1.8	15	47	0.01	0.89	187	8	2
Mixed Lipids												
cPnA, DMPC/DPPC 1:1	45	1.3	3.8	0.11	0.2	3.1	5	0.02	0.26	54	4	4
	28	3.8	12	0.27	0.2	4.5	13	0.01	0.67	1100	28	27
	15	4.1	21	0.19	2.4	8.9	25	0.06	0.62	3300	55	27
tPnA, DMPC/DPPC 1:1	45	2.1	6	0.43	0.2	2.7	7	0.03	0.34	191	5	3
	28	6.4	25	0.18	1.6	7.6	26	0.01	0.79	1400	47	47
	15	7.4	38	0.13	3.2	13	40	0.03	0.80	2500	46	27

model, negative Δ and Λ values that decrease with modulation frequency were measured in the presence of heterogeneous rotational motion. Anisotropic or hindered rotation of a single fluorophore gives *only* positive Δ and Λ values that *increase* with modulation frequency, so that measurement of negative Δ and decreasing Λ is indicative of ground-state rotational heterogeneity.

Errors in values of Δ and Λ are smallest in the middle range of frequencies. At low modulation frequencies, there is little shift in phase or change in modulation amplitude, leading to a measurement of Δ (Λ) as the difference (ratio) between two numbers of nearly equal magnitude. At high modulation frequencies, errors in Δ and Λ are large because of the strong demodulation of emitted fluorescence.

The precision to which fitted parameters can be determined by the DHR model is given by the calculated errors in the fitted parameters; large errors in fitted parameters indicate little sensitivity of χ^2 to changes in parameter values. The sensitivity of the fit to a ±20% change in fitted parameters is shown graphically in Figure 1B. The simulations indicate stronger sensitivity of the predicted curve shapes on r_∞ and g_1 than on τ_c, and that a 20% change in individual parameter values gives a significant change in predicted Δ and Λ values.

Parinaric Acids in Pure Phospholipids. Lifetime and differential polarization studies were performed using cPnA and tPnA in pure DMPC and pure DPPC vesicles above, near, and below their phase transition temperatures. In the next section, experiments are described using mixed phospholipids having distinct gel and fluid domains to determine whether the DHR model could be used to resolve parinaric acid rotational parameters in separate domains in a complex membrane system.

Table II, top, gives lifetimes of cPnA and tPnA in DMPC and DPPC liposomes. In all cases, a fit of two lifetimes was significantly better than a fit of one lifetime ($p < 0.001$). At 45 °C, above the phase transition temperature (T_c) of both DMPC (T_c = 24 °C) and DPPC (T_c = 41 °C), the lifetime data of cPnA and tPnA are fit by two lifetimes; inclusion of a third lifetime does not significantly improve the χ^2 value ($p < 0.01$). At temperatures below 45 °C, some lifetime data are better described by three lifetimes; however, >96% of the fluorescence signal is described by two lifetimes, with the third lifetime of low fractional intensity and typically <2 ns. For both cPnA and tPnA, the lifetimes increase with decreasing temperature.

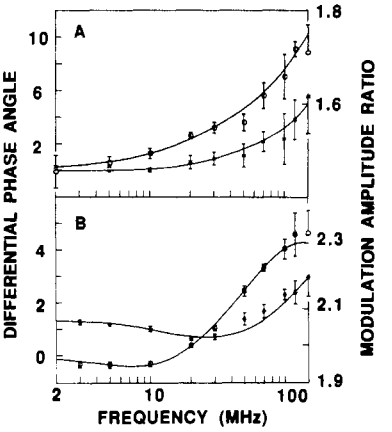

FIGURE 2: Differential phase angles (O) and modulation amplitude ratios (asterisks) for tPnA in DMPC. (A) T = 45 °C. (B) T = 20 °C. The lines represent the least-squares fit of the DHR model to the data; fit parameters are given in Table III, top.

The most striking observation from the lifetime data is the appearance of a long-lifetime component (10–22 ns for cPnA and 27–47 ns for tPnA) at temperatures below the lipid-phase transition, which has been associated with fluorophore in gel-phase lipid (Sklar et al., 1977; Parasassi et al., 1984). At 20 °C, the lifetimes of cPnA and tPnA in DMPC are shorter than those in DPPC.

The results from fitting differential polarization data for cPnA and tPnA in pure DMPC and pure DPPC by the rotational models are given in Table III, top; an example of the fit is given in Figure 2. In all cases, the DHR model fit significantly better than either the isotropic (P = 0.0001–0.001) or the single hindered rotator model (P = 0.001–0.09). At 45 °C, the fit by the DHR model or by the anisotropic rotator model with two correlation times could not be distinguished on the basis of χ^2 values; at temperatures below 45 °C, the DHR model fit significantly better. As for the two-compartment cuvette studies in the previous section, the correlation times obtained by a fit of the DHR model are not well determined.

Table III: Parameters from Fit of Double Hindered Rotator Model to Differential Polarization Data[a]

probe, lipid	temp (°C)	$r_{\infty 1}$	$r_{\infty 2}$	τ_{c1} (ns)	τ_{c2} (ns)	g_1	χ^2 DHR	χ^2 SHR	χ^2 ISO	χ^2 ANISO
Pure Lipids										
cPnA, DMPC	45	0.15 ± 0.04	0.053 ± 0.004	0.37 ± 0.18	0.22 ± 0.08	0.71 ± 0.18	0.65	2.02	36.4	0.66
	32	0.11 ± 0.03	0.10 ± 0.10	0.06 ± 0.10	1.3 ± 0.3	0.39 ± 0.09	0.27	1.43	125	1.13
	20	0.094 ± 0.004	0.28 ± 0.03	2.0 ± 0.3	0.00 ± 0.010	0.73 ± 0.10	14.9	32.9	538	41.4
cPnA, DPPC	45	0.06 ± 0.02	0.08 ± 0.01	0.98 ± 0.13	0.0 ± 0.08	0.75 ± 0.05	0.49	3.35	182	0.66
	32	0.25 ± 0.01	0.34 ± 0.01	0.45 ± 0.17	0.25 ± 1	0.68 ± 0.03	0.79	11.37	125	11.37
	20	0.22 ± 0.01	0.33 ± 0.01	0.83 ± 0.08	0.00 ± 0.07	0.21 ± 0.01	0.30	4.98	3587	1050
tPnA, DMPC	45	0.11 ± 0.01	0.04 ± 0.02	0.43 ± 0.06	0.4 ± 0.2	0.87 ± 0.03	0.48	1.6	38	0.64
	32	0.0 ± 0.5	0.12 ± 0.01	1 ± 3	0.4 ± 3	0.75 ± 0.15	1.2	1.4	67	1.2
	20	0.23 ± 0.01	0.31 ± 0.01	0.5 ± 0.2	0.5 ± 0.3	0.34 ± 0.03	0.72	3.6	230	1300
tPnA, DPPC	45	0.15 ± 0.04	0.12 ± 0.01	0.4 ± 0.4	0.3 ± 0.4	0.6 ± 0.3	0.39	0.79	120	0.37
	32	0.05 ± 0.06	0.32 ± 0.01	0 ± 1	0 ± 0.6	0.05 ± 0.09	1.5	7.4	2000	1800
	20	0.25 ± 0.02	0.33 ± 0.01	4.3 ± 1.6	0.03 ± 0.30	0.09 ± 0.01	4.4	5.0	1300	1000
Mixed Lipids										
cPnA, DPPC/DMPC	45	0.13 ± 0.08	0.065 ± 0.006	0.5 ± 0.6	0.4 ± 0.2	0.5 ± 0.2	0.37	0.76	30	0.38
	28	0.005 ± 0.001	0.23 ± 0.01	2.4 ± 0.1	0.12 ± 0.02	0.41 ± 0.01	4.0	14	910	18
	15	0.13 ± 0.01	0.31 ± 0.03	3.0 ± 0.1	0.00 ± 0.04	0.25 ± 0.01	0.73	2.4	500	650
tPnA, DPPC/DMPC	45	0.14 ± 0.02	0.04 ± 0.02	0.39 ± 0.11	0.3 ± 0.4	0.88 ± 0.04	0.68	1.7	34	0.73
	28	0.21 ± 0.04	0.31 ± 0.01	0.52 ± 0.3	0.00 ± 0.2	0.40 ± 0.17	1.6	74	11000	3700
	15	0.26 ± 0.01	0.32 ± 0.01	0.0 ± 0.5	0.15 ± 0.01	0.004 ± 0.002	0.58	0.52	250	6900

[a] For the fit, lifetimes were held constant to values determined in Table II; r_0 was held fixed at 0.36.

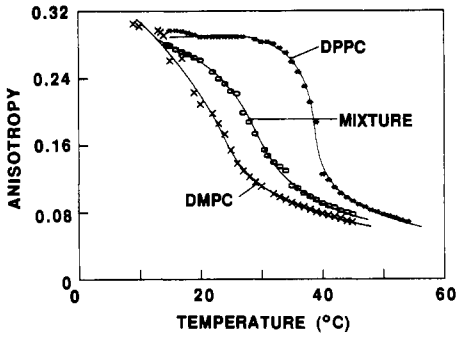

FIGURE 3: Steady-state anisotropy of DPH in DPPC, DMPC, and a 1:1 mixture of DMPC/DPPC as a function of temperature.

The appearance of a long-lifetime component for cPnA and tPnA in DMPC at 20 °C and in DPPC at 32 and 20 °C (temperatures below the phase transitions of the lipids) is correlated with an increase in r_∞ to a value ~0.3, confirming that the long-lifetime component arises from probe in gel-phase lipid.

Parinaric Acids in Mixed Phospholipids. To examine parinaric acid lifetimes and rotational motion in a two-phase system, experiments were done with a 1:1 mixture of DPPC and DMPC, a mixture which exhibits lateral-phase separation. The temperature at which two phases coexist for this mixture was determined by measuring the steady-state anisotropy (r) of DPH as a function of temperature. The results, shown in Figure 3, indicate a phase transition near 40 °C for pure DPPC and near 25 °C for pure DMPC. As predicted from the phase diagram of DMPC/DPPC mixtures, the apparent phase transition is broadened in the mixture because of lateral-phase separation. Lifetime and differential polarization measurements were done at 15 °C to probe a single, solid lipid phase, at 45 °C to probe a single, fluid lipid phase, and at 28 °C to probe a two-phase lipid system.

Fluorescence lifetimes for cPnA and tPnA in mixed phospholipids are given in Table II, bottom. As was the case for pure lipids, parinaric acids in mixed lipids exhibit either two lifetimes or three lifetimes with one lifetime short and/or of low fractional intensity. At 45 °C, parinaric acid lifetimes are similar in pure DMPC and DPPC (Table II, top); not surprisingly, the lifetimes in the DMPC/DPPC lipid mixture

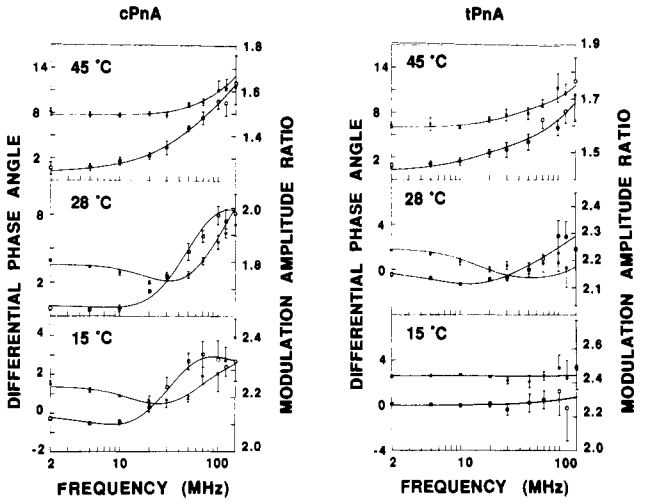

FIGURE 4: Differential phase angles (O) and modulation amplitude ratios (asterisks) of cPnA and tPnA in a 1:1 mixture of DMPC/DPPC at various temperatures. The lines represent a fit of the DHR model to the data; fitted parameters are given in Table III, bottom.

are approximately equal to those in the pure lipid. At 20 °C, parinaric acids have a shorter lifetime in DMPC than in DPPC; in the mixed lipid system, the measured lifetimes are in between those in the pure lipids. For pure lipids at intermediate temperatures, parinaric acid lifetimes vary greatly because DMPC is above its phase transition temperature and DPPC is below its phase transition temperature. In mixed lipids at intermediate temperatures, measured lifetimes are in between those measured in the pure lipids.

Differential polarization data for parinaric acids in the mixed lipid system are shown in Figure 4. At 45 °C, Δ values are positive, and Λ values increase with increasing frequency, suggesting that ground-state rotational heterogeneity may not be necessary to describe parinaric acid motion in mixed lipids at temperatures in which there is only one phase present. However, at 28 °C, a temperature in which two lipid phases coexist, the data clearly show departure from that predicted from single ground-state rotator models: Δ values are negative and/or Λ decrease with increasing frequency. Similar data were obtained with the two-compartment cuvette (Figure 1) and suggest that both tPnA and cPnA detect the presence of

Table IV: Parameters from Fit of Double Hindered Rotator Model to Differential Polarization Data for cPnA in Red Cell Ghosts

temp (°C)	τ_{f1} (ns)	τ_{f2} (ns)	$r_{\infty 1}$	$r_{\infty 2}$	τ_{c1} (ns)	τ_{c2} (ns)	g_1	χ^2 DHR	χ^2 SHR	χ^2 ISO	χ^2 ANISO
40	2.4	7.6	0.07 ± 0.1	0.11 ± 0.01	4 ± 4	0.091 ± 0.06	0.26 ± 0.09	0.40	7.3	1100	3.1
35	5.6	11.6	0.13 ± 0.01	0.12 ± 0.01	2.2 ± 0.05	0.12 ± 0.03	0.28 ± 0.04	0.40	9.0	1900	5.7
30	2.9	9.7	0.02 ± 0.13	0.12 ± 0.01	10 ± 5	0.13 ± 0.03	0.26 ± 0.02	0.96	17	1100	6.9
25	3.4	12.3	0.17 ± 0.01	0.12 ± 0.01	0 ± 0.01	0.88 ± 0.02	0.53 ± 0.01	1.6	34	8700	7.6
20	4.3	14.9	0.07 ± 0.14	0.13 ± 0.01	8 ± 7	0.16 ± 0.05	0.33 ± 0.02	0.85	19	1600	9.4
15	5.4	16.0	0.09 ± 0.02	0.12 ± 0.01	0.18 ± 0.04	3.8 ± 0.6	0.58 ± 0.03	0.86	120	120	34

two phases in the mixed lipid system at 28 °C. At 15 °C, the differential polarization data for cPnA suggest that this probe still detects two phases. The data for tPnA at 15 °C are nearly frequency-independent over the range 2–150 MHz, indicating very slow and/or very hindered motion for tPnA at this temperature.

The parameters and χ^2 values obtained from a fit of the rotator models to differential polarization data in mixed lipid systems are given in Table III, bottom. At all temperatures, the DHR model fit better than the isotropic or SHR model. As was the case for pure lipids, the DHR model and the anisotropic rotator model gave equally good fits at 45 °C, while at lower temperatures, the DHR model fit the data better. The r_∞ values determined for the mixed lipids were generally intermediate between those obtained in the pure lipids separately.

Parinaric Acids in Erythrocyte Ghost Membranes. To investigate multiple lipid phases in a biological membrane, differential polarization and lifetime data were obtained for cPnA in human erythrocyte ghost membranes in the temperature range 15–40 °C. Erythrocyte ghosts were chosen because they can be prepared with high purity and have been characterized extensively with respect to temperature-dependent transport properties and enzyme function. Analysis of the lifetime data indicated that two lifetimes are adequate to describe the phase/modulation data for cPnA at all temperatures; inclusion of a third lifetime did not improve the χ^2 value significantly. At low temperatures, a long-lifetime component was observed (12–18 ns), similar to that in pure phospholipids below the phase transition temperature.

Δ and Λ values for cPnA in ghosts are given in Figure 5. Lifetimes, χ^2 values for fits of rotator models, and parameters for a fit of the DHR model to the differential polarization data are given in Table IV. The DHR model fits the data significantly better than the other rotational models; however, unlike the data in pure phospholipids, there was no evidence for a distinct phase transition.

Discussion

The purpose of this study was to evaluate the application of multifrequency phase-modulation fluorometry for determination of the rotational parameters of fluorophores rotating in separate environments. This is an important application in cell and membrane biophysics because multiple lipid domains having unique responses to hormonal and other stimuli are present in biological membranes. Our strategy was to develop an anisotropy decay model for the isotropic hindered rotation of two independent species which might correspond physically to one fluorophore rotating in two separate environments, or to two noninteracting fluorophores rotating in a single environment. The mathematical form of the anisotropy decay profile contained a sum of two noninteracting isotropic hindered rotators, each with an exponential decay of total fluorescence. We did not evaluate other complex anisotropy decay profiles, such as the multiple exponential decay expected for a fluorophore attached to a rapidly rotating arm of a protein (Ludescher et al., 1987), because they were less plausible physically or the limited resolution of the data did not justify inclusion of additional parameters. We did not evaluate pulsed lifetime methods, nor did we use alternative approaches for the analysis of phase-modulation data such as the "sine–cosine transform method" (Van der Meer et al., 1987; Pottel et al., 1987) or global analysis methods (Lakowicz et al., 1987). With improved instrumentation and global analysis methods, it may be possible to evaluate anisotropy decay models containing continuous distributions in rotational parameters.

The ability of the model to retrieve rotational parameters from two rotators was validated experimentally by using a two-compartment cuvette containing fluorophores having different rotational parameters. The model was applied to analysis of parinaric acid rotation in pure and mixed phospholipid liposome systems, and then in intact red cell membranes. The results show that rotational parameters can be resolved successfully from two independent rotators; however, current methodological limitations restrict the accuracy of parameter determination as discussed below. Because of the relatively long parinaric acid lifetimes and the lack of wavelength-dependent dynamic parameters, use of high-frequency modulation by a mode-locked laser system (Lakowicz et al., 1986) would be unlikely to improve significantly the accuracy of rotational parameter determination.

cis- and *trans*-parinaric acids were selected as the lipid probes for membrane studies because of their strong dependence of lifetime on membrane phase state (James et al., 1987; Parasassi et al., 1984; Sklar et al., 1977). Parinaric acids have been used successfully in a large number of systems to study membrane phase transitions (Alfsen et al., 1984; James et al., 1987; Illsley et al., 1987; Parasassi et al., 1984; Sklar et al., 1979a,b; Soulages et al., 1988) and, by use of dynamic methods, to resolve the domain structure of artificial and biological membranes (Illsley et al., 1987, 1988; Schroeder, 1983; Schroeder et al., 1987). In addition, the peak excitation wavelength for these fluorophores corresponds exactly to the 325-nm line of the He–Cd laser. Although the details of fluorescence lifetime decay kinetics have been reported in some studies to be complex, we nonetheless concluded that the important advantages for use of parinaric acids outweighed the potential difficulties of a complex decay profile.

The steady-state anisotropy, r, of cPnA and tPnA in lipid bilayers has been studied for a series of lipids and temperatures. For cPnA, r values have been reported in the range 0.09–0.13 for lipids in the liquid-crystalline state and 0.3–0.35 in the gel phase (Sklar et al., 1979a,b; Gallay & Vincent, 1986; Rujanavech et al., 1986). For tPnA, r values are 0.11–0.17 for lipids in the liquid-crystalline state and 0.22–0.36 in the gel phase (Sklar et al., 1979a,b; Souzu, 1986; Gallay & Vincent, 1986). Studies of the temperature dependence of r for cPnA and tPnA in lipid mixtures revealed broadening of the heating and cooling curves in regions of phase space where lateral-phase separation occurred, similar to our data for DPH (Figure 3). These results indicate that r values of PnA are sensitive to the physical state of the lipid and can be used to monitor

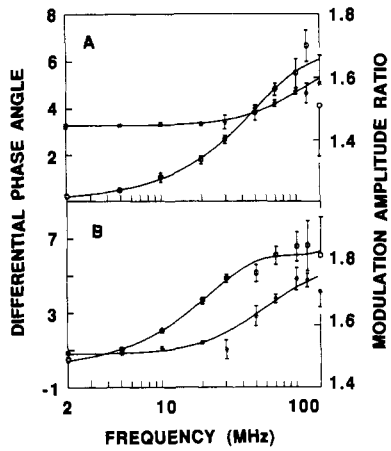

FIGURE 5: Differential phase angles (O) and modulation amplitude ratios (asterisks) of cPnA in human erythrocyte ghost membrane. (A) T = 40 °C; (B) T = 20 °C.

phase transitions. However, because r values depend in general on the fluorescence lifetime, rates of rotational motion, and the degree of motional hindrance, r values can be used only semiempirically to study phase behavior of lipids.

To obtain a more detailed description of PnA motion, and hence of the bilayer physical state, time-resolved or multifrequency phase/modulation measurements are necessary. Several recent studies have used this approach to study PnA motion in bilayers made from synthetic lipids and lipids extracted from biological membranes (Schroeder et al., 1987; Gallay & Vincent, 1986; Rujanavech et al., 1986; Wolber & Hudson, 1981) and from biological membranes including synaptic plasma vesicles and coated vesicles (Schroeder et al., 1987; Wood et al., 1986; Alfsen et al., 1984). All reported measurements have yielded two or more lifetimes for PnA in membranes. For pure phospholipids in the liquid-crystalline state, r_∞ values of 0.04–0.07 have been reported for cPnA and tPnA; r_∞ values of 0.30–0.34 are found for cPnA in gel-phase lipids. In PC/cholesterol vesicles, complex anisotropy decays were measured by Ludescher et al. (1987) using pulsed methods, where the form for $r(t)$ was strongly suggestive of ground-state rotational heterogeneity. In the biological membranes that have been studied, r_∞ values ~0.15 (cPnA) and ~0.20 (tPnA) have been reported in the temperature range 30–37 °C. Wolber and Hudson (1981) showed that cPnA and tPnA exhibit a single lifetime in cyclohexanol, implying that the multiexponential character found in membranes is not an intrinsic property of the fluorophore but may represent heterogeneity in the lipid environment of the probe. Despite this implication, most studies of PnA motion in membranes have used the single hindered rotator model or anisotropic rotator model to analyze time-resolved or phase/modulation data with a single, intensity-weighted average lifetime.

The work presented here represents an extension of available rotational models that explicitly includes rotational heterogeneity arising from lipid-phase heterogeneity. The phase/modulation data for PnA in DMPC/DPPC (Figure 4) at temperatures in which lateral-phase separation has occurred show negative Δ and decreasing Λ, clearly indicating the presence of PnA rotational heterogeneity in this system. Rotational heterogeneity is also observed for cPnA in the lipid mixture at temperatures in which only solid phase is present. Similar results were found for tPnA in DPPC above T_c by Wolber and Hudson (1981). Using time-resolved measurements, they found that the apparent r_∞ increased with time, suggesting that tPnA senses at least two environments. We conclude that analysis of fluorophore rotation in a complex lipid environment requires the use of an anisotropy decay model with rotational heterogeneity. The data reported here show that multifrequency phase-modulation data give useful information to resolve the complex rotation of PnA in artificial systems and, potentially, in simple biological membranes.

ACKNOWLEDGMENTS

We thank Dr. Nicholas P. Illsley for computer programming and Dr. Rengao Ye for the erythrocyte ghost preparation.

Registry No. cPnA, 593-38-4; tPnA, 18841-21-9; DPPC, 2644-64-6; DMPC, 13699-48-4.

REFERENCES

Alfsen, A., de Paillerets, C., Nandi, P. K., Lippoldt, R. E., & Edelhoch, H. (1984) *Eur. Biophys. J. 11*, 129–136.

Bevington, P. R. (1969) *Data Reduction and Error Analysis for the Phsical Sciences*, McGraw-Hill, New York.

Cantor, C. R., & Schimmel, P. R. (1980) *Biophysical* Chemistry, Part II, pp 463–465, W. H. Freeman, New York.

Gallay, J., & Vincent, M. (1986) *Biochemistry 25*, 2650–2656.

Illsley, N. P., Lin, H. Y., & Verkman, A. S. (1987) *Biochemistry 26*, 446–454.

Illsley, N. P., Lin, H. Y., & Verkman, A. S. (1988) *Biochemistry 27*, 2077–2083.

James, D. R., Turnbull, J. R., Wagner, W. R., & Petersen, N. O. (1987) *Biochemistry 26*, 6272–6277.

Lakowicz, J. R., Prendergast, F. G., & Hogen, D. (1979) *Biochemistry 18*, 508–519.

Lakowicz, J. R., Cherek, H., & Balter, A. (1981) *J. Biochem. Biophys. Methods 5*, 131–146.

Lakowicz, J. R., Laczko, G., Cherek, H., Gratton, E., & Limkeman, M. (1984) *Biophys. J. 46*, 463–477.

Lakowicz, J. R., Cherek, H., & Badri, M. P. (1985) *Biochemistry 24*, 376–382.

Lakowicz, J. R., Laczko, G., & Gryczysnki, I. (1986) *Rev. Sci. Instrum. 57*, 2499–2506.

Lakowicz, J. R., Cherek, H., Gryczynski, I., Joshi, N., & Johnson, M. L. (1987) *Biophys. Chem. 28*, 35–50.

Ludescher, R. D., Peting, L., Hudson, S., & Hudson, B. (1987) *Biophys. Chem. 28*, 59–75.

Parasassi, T., Conti, F., & Gratton, E. (1984) *Biochemistry 23*, 5660–5664.

Pottel, H., Van der Meer, B. W., Herreman, W., & Depauw, H. (1987) *Eur. Biophys. J. 15*, 47–58.

Prendergast, F. G., Haugland, R. P., & Callahan, P. J. (1981) *Biochemistry 20*, 7333–7338.

Rujanavech, C., Henderson, P. A., & Silbert, D. F. (1986) *J. Biol. Chem. 261*, 7204–7214.

Schroeder, F. (1983) *Eur. J. Biochem. 132*, 509–516.

Schroeder, F., Gorka, C., Williamson, L. S., & Wood, W. G. (1987) *Biochim. Biophys. Acta 902*, 385–393.

Sklar, L. A. (1980) *Mol. Cell. Biochem. 32*, 169–177.

Sklar, L. A., Hudson, B. S., & Simoni, R. D. (1977) *Biochemistry 16*, 819–828.

Sklar, L. A., Miljanich, G. P., Bursten, S. L., & Dratz, E. A. (1979a) *J. Biol. Chem. 254*, 9583–9591.

Sklar, L. A., Miljanich, G. P., & Dratz, E. A. (1979b) *Biochemistry 18*, 1707–1716.

Steck, T. L., & Kant, E. (1974) *Methods Enzymol. 31*, 172–177.

Soulages, J. L., Rimoldi, O. J., & Brennder, R. R. (1988) *J. Lipid Res. 29*, 172–182.

Souzu, H. (1986) *Biochim. Biophys. Acta 861*, 353–360.

Van der Meer, B. W., Pottel, H., & Herreman, W. (1987) *Eur. Biophys. J. 15*, 35–45.
Weber, G. (1977) *J. Chem. Phys. 66*, 4081–4091.
Wolber, P. K., & Hudson, B. S. (1981) *Biochemistry 20*, 2800–2810.
Wood, W. G. Gorka, C., Williamson, L. S., Strong, R., Sun, A. Y., Sun, G. Y., & Schroeder, F. (1986) *FEBS Lett. 205*, 25–28.

Effects of Temperature and Glycerol on the Resonance Raman Spectra of Cytochrome *c* Peroxidase and Selected Mutants†

Giulietta Smulevich,*,‡ Anna R. Mantini,‡ Ann M. English,*,§ and J. Matthew Mauro‖

Dipartimento di Chimica, Università di Firenze, Via G. Capponi 9, 50121 Firenze, Italy, Department of Chemistry, Concordia University, Montreal, Quebec, Canada H3G 1M8, and Department of Chemistry, University of California, San Diego, La Jolla, California 92093

Received December 13, 1988; Revised Manuscript Received February 23, 1989

ABSTRACT: The high-frequency resonance Raman spectra of Fe^{III} yeast native cytochrome *c* peroxidase (CCP) and five of its mutants [CCP(MI), Phe-51, Leu-48, Lys-48, Asn-235, and Phe-191] were recorded in phosphate buffer, pH 7.0, and in glycerol/phosphate mixtures at 295 and 10 K. Glycerol induces heme coordination changes in some of the CCP mutants at room temperature. It apparently weakens the binding of the Fe atom to ligands in the distal heme cavity and drives the heme toward the 5-coordinate, high-spin state. At 10 K, native CCP and all the mutants (except Phe-51 which remains 6-coordinate, high-spin) show various distributions of spin and coordination states which differ from those observed at 295 K. Upon cooling in phosphate buffer, pH 7, and to a much lesser extent in 66% glycerol/phosphate, an internal strong-field ligand is coordinated to the Fe. A likely candidate is H_2O-595, which could become a strong-field ligand on H-bonding and/or proton transfer to H_2O-648, and/or the distal His-52. However, distal His-52 itself cannot be ruled out as the coordinating ligand considering that the Phe-51 mutant, which binds H_2O-595 at room temperature, does not show a large 6-coordinate, low-spin component at 10 K like the other mutants. These results clearly indicate that the Fe coordination in CCP and its mutants is sensitive to both temperature and solvent composition.

Changes in the electronic absorption and magnetic properties of hemoproteins versus temperature have been extensively reported [see Beetlestone and George (1964) and references cited therein and Iizuka and Kotani (1969a,b) and references cited therein]. Such changes were mainly ascribed to thermal mixtures of low- and high-spin states, rather than to changes in the axial ligation of the iron atom. However, recent reports (Schulz et al., 1984; Evangelista-Kirkup et al., 1985; Manthey et al., 1986; Andersson et al., 1987) have suggested that a number of hemoproteins may undergo freezing-induced conformational changes, which cause spin and coordination transitions due to the reversible binding of a sixth ligand to the iron atom. Glycerol addition to solutions of cytochrome *c* peroxidase (CCP)[1] (Yonetani & Anni, 1987) and HRP (Schulz et al., 1984) prevents the high-spin (hs) to low-spin (ls) transition observed on cooling these peroxidases. Since glycerol is known to stabilize the tertiary structure of proteins (Gekko & Timasheff, 1981), this suggests that a change in ligation occurs on freezing.

The effects of temperature on the absorption (Yonetani et al., 1966) and EPR spectra (Yonetani & Anni, 1987; Hori & Yonetani, 1985) and magnetic susceptibility of CCP (Iizuka et al., 1968) have been studied extensively by Yonetani and co-workers. On the basis of their results, they originally proposed that CCP was a pH-dependent mixture of acidic and alkaline forms between pH 4 and 8. They further concluded that *both* the acidic (pH 5) and alkaline (pH 7) forms possessed hs and ls states in thermal equilibrium; the alkaline form was ls below 173 K and became increasingly hs on heating, whereas the acidic form was hs below 173 K and showed an increasing ls component at high temperatures (Iizuka et al., 1968). Thus, while their visible absorption spectra were similar at room temperature, at 83 K the acidic and alkaline forms showed typical hs and ls spectra, respectively, and a pK_a of ~6 was estimated for the acidic–alkaline transition at 83 K.

Resonance Raman (RR) spectroscopy is a useful probe of heme structure since the Raman frequencies are sensitive to the coordination number as well as the spin state of the iron (Smulevich et al., 1988). Recently, Yonetani and co-workers reported the RR spectra of Fe^{III} CCP (Hashimoto et al., 1986). From these data, they concluded that CCP was a pH-dependent mixture of 6-coordinate (6-c) and 5-coordinate (5-c) hs species at room temperature. Since the 6-c form was dominant at pH 5, and the 5-c form at pH 7, these structures were assigned to the previously proposed acidic and alkaline forms of CCP, respectively, and a pK_a of 5.5 was obtained for the 6-c ⇌ 5-c transition at room temperature [see Figure 5

† This research was supported by the Italian Consiglio Nazionale delle Richerche and Ministero della Pubblica Istruzione (to G.S.), NSERC (Canada) Grant A1530 (to A.M.E.), NATO Grant 86/0453 (to G.S. and A.M.E.), and NSRA Postdoctoral Fellowship PHS GM 10292-02 (to J.M.M.).

* Author to whom correspondence should be addressed.
‡ Università di Firenze.
§ Concordia University.
‖ University of California, San Diego.

[1] Abbreviations: CCP, cytochrome *c* peroxidase; HRP, horseradish peroxidase; RR, resonance Raman; EPR, electron paramagnetic resonance; ls, low spin; hs, high spin; 5-c, 5-coordination; 6-c, 6-coordination.

0006-2960/89/0428-5058$01.50/0